

Origin of the unusual strong suppression of low-frequency antiferromagnetic fluctuations in underdoped $\text{HgBa}_2\text{CuO}_{4+\delta}$

Jia-Wei Mei,¹ Alexey A. Soluyanov,¹ and T. M. Rice^{1,2}

¹*Institute for Theoretical Physics, ETH Zürich, 8093 Zürich, Switzerland*

²*Brookhaven National Laboratories, Upton, New York, USA*

(Received 8 September 2013; revised manuscript received 8 April 2014; published 22 April 2014)

Generally strong charge and magnetic inhomogeneities are observed in NQR/NMR experiments on underdoped cuprates. It is not the case for the underdoped $\text{HgBa}_2\text{CuO}_{4+\delta}$, the most symmetric and highest T_c single layer cuprate, whose magnetic inhomogeneity is strongly suppressed. Also neutron scattering experiments reveal a unique pair of weakly dispersive magnetic modes in this material. We propose that these special properties stem from the symmetric positioning of the O dopants between adjacent CuO_2 layers that lead to a strong superexchange interaction between a pair of hole spins. In this Rapid Communication we present a theoretical model, which gives a consistent explanation to the anomalous magnetic properties of this material.

DOI: [10.1103/PhysRevB.89.161115](https://doi.org/10.1103/PhysRevB.89.161115)

PACS number(s): 74.62.Dh, 74.20.-z, 74.25.Jb, 74.62.Bf

The single layer cuprate $\text{HgBa}_2\text{CuO}_{4+\delta}$ (Hg1201) has not only the most symmetric crystal structure and the highest transition temperature, with a maximum value of 97 K, but it also displays marked deviations in key properties from other single layer cuprate superconductors. NMR experiments on underdoped Hg1201 observe the usual charge disorder, but the standard magnetic disorder is absent [1–4]. In addition, neutron scattering finds two finite energy local excitations not observed elsewhere [5,6]. Li *et al.* [5,6] interpreted these two triplet modes as a fingerprint of circulating orbital currents within the CuO_6 octahedra. We propose an alternative explanation which relates these triplet modes to the suppression of magnetic disorder in the NMR experiments. Finally, although the O atom is strongly electronegative and generally favors an ionic state O^{2-} , a substantial fraction of the holes is not inserted into the CuO_2 planes and remains on the dopant site (O^d) [7,8]. Understanding the origin of these special features in the most ideal cuprate is a highly relevant challenge to theory. In this Rapid Communication we take a closer look at the actual crystal structure of Hg1201 and propose a consistent explanation of all these anomalies.

In Hg1201 the O dopants enter the Hg layer, which is symmetrically placed halfway between neighboring CuO_2 layers. As a result the local enhancement of the hole density will be equal in the layers above and below O^d . This structure is clearly different from other single layer cuprates, e.g., $\text{La}_{2-x}\text{Sr}_x\text{CuO}_4$, where the dopant injects a single hole into a single nearby layer. A localized single hole in a CuO_2 layer is generally accompanied by a free spin and RKKY-like coupling of the free spin to neighboring Cu nuclei causes the magnetic disorder observed in NMR experiments [1]. As will be discussed later, we propose that in Hg1201 this mechanism is absent because the free spins are bound into singlets.

The more complex structure of the dopant O ion in Hg1201 requires a more detailed investigation of the charge distribution and accompanying spin distribution around the dopant site. Diffuse neutron scattering experiments by Jorgensen and co-workers [7] reported two different sites for the O dopant (O^d) in the Hg layer. At higher densities O^d is predominantly at the O(3) site, which is symmetrically placed at the center of a square of Hg ions. But at lower densities, O^d chooses

predominantly an asymmetric site, O(4), lying close to a single Hg ion. In this case a single strong Hg-O(4) bond of ~ 2 Å in length forms, whereas the larger Hg-O separation from the O(3) site greatly weakens hybridization between the planar $2p$ states of the O ions and the neighboring Hg ions.

The electronic structure of the O^d can be investigated using first-principles local-density approximation (LDA) calculations for a periodic supercell containing a single O^d . Supercell LDA calculations for the symmetric O(3) site were carried out by Ambrosch-Draxl *et al.* [9], who found an essentially ionic structure for this weakly hybridized O^d but one with only partial occupancy of the uppermost O-valence states. These states overlap in energy with the uppermost CuO_2 layer states leading to a hole density which is shared between the O^d and the neighboring CuO_2 layers. As remarked above, a reduced hole concentration in the layers is found experimentally [7,8]. In the case of the O(4) site, we have performed LDA calculations [10] for a periodic eight-unit supercell containing one occupied O(4) site. The local density of states (see Fig. 1) has a filled bonding state below a partially filled antibonding state, indicating that O(4) also has holes distributed between the O^d site in the Hg plane and sites in the nearby CuO_2 planes, again in agreement with experiment.

We now turn to the analysis of the spin states and magnetic properties resultant from these two possible positions of O^d . For this purpose we examine how the spins of the holes moving in the adjacent CuO_2 planes are coupled via superexchange paths through the O^d . The suppressed magnetic inhomogeneity suggests that the two holes form a singlet ground state. In this case the two weakly dispersive magnetic modes in Hg1201 observed with neutron scattering [5,6] can be attributed to the triplet excited states above such a ground state. The analysis of spin correlations of dopant holes localized around O^d that we present below supports such a scenario especially for the O(4) dopant location.

We start our analysis by considering electrons moving in the CuO_2 planes. These are described by a three-band Hubbard model containing the $\text{O}(1)-2p_x, 2p_y$ and $\text{Cu}-3d_{x^2-y^2}$ orbitals. Early on it was shown that this description can be reduced

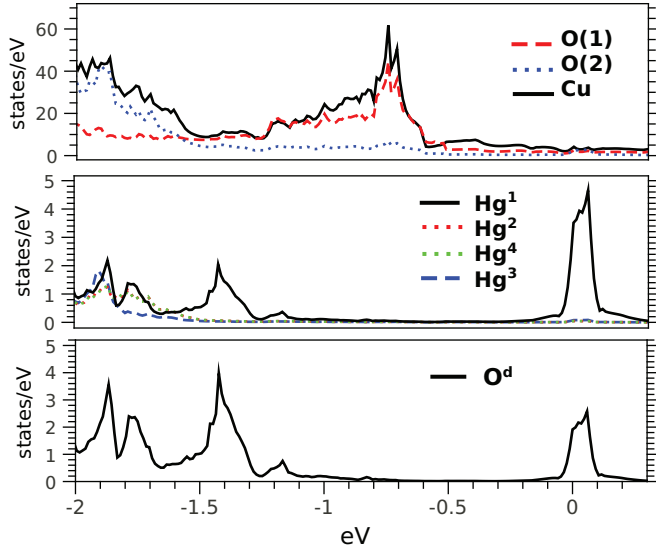


FIG. 1. (Color online) Projected DOS of a single supercell with the chemical potential set to zero for $\delta = 0.125$ with the oxygen dopant O^d at the O(4) site. Top panel: CuO_2 layer contribution to DOS, O(1) planar, O(2) apical O sites. Midpanel: Projected DOS of Hg atoms in the unit cell containing O^d . Hg¹ (Hg³) are the nearest (furthest from) to O^d , Hg^{2,4} remaining Hg sites at the corners of the Hg₄ square. Bottom panel: Projected DOS at the dopant O^d located at the O(4) site. See Ref. [9] for the results for the case O^d is at the O(3) site.

to a one-band Hubbard model with a zero as the on-site energy [11,12]

$$H_0 = -t \sum_{nn} (c_i^\dagger c_j + \text{H.c.}) - t' \sum_{nnn} (c_i^\dagger c_j + \text{H.c.}) + \sum_i U n_{i\uparrow} n_{i\downarrow}. \quad (1)$$

Typical parameters for a CuO_2 plane were estimated by Hybertsen *et al.* [12], who found values for nearest (nn) and next-nearest (nnn) neighbor hoppings t and t' , respectively, and the on-site Hubbard repulsion U to be

$$t = 0.43 \text{ eV}, \quad t'/t = -0.16, \quad U/t = 12.6. \quad (2)$$

Note, however, that if we assume the attractive potential of the O^d dopant confines the hole motion to a Cu_4 plaquette, there are just four sites and the kinetic energy is reduced. If we still take $U/t = 12.6$, we are too close to the infinite U limit where a Nagaoka effect applies, leading to a high spin $S = 3/2$ ground state [13] for three electrons on a Cu_4O_4 plaquette. However, a more physical low spin value can be obtained by using a smaller value $U/t = 6.0$, giving a ground state with $S = 1/2$. This is the simplest model to describe both charge and magnetic inhomogeneities similar to that of a hole localized in the CuO_2 plane around a Sr^{2+} dopant in $\text{La}_{2-x}\text{Sr}_x\text{CuO}_4$ [1,14].

Next we model the superexchange path coupling the spins of a pair of holes in Cu_4O_4 plaquettes above and below a O^d dopant. The hopping of the holes from the planes to the O^d site leads to a superexchange interaction. The smallest local model to describe this behavior is a $\text{Cu}_4\text{O}_4\text{-O}^d\text{-Cu}_4\text{O}_4$ cluster using a one-band Hubbard model to describe each Cu_4O_4 plaquette. The O(4) dopant state is then approximated

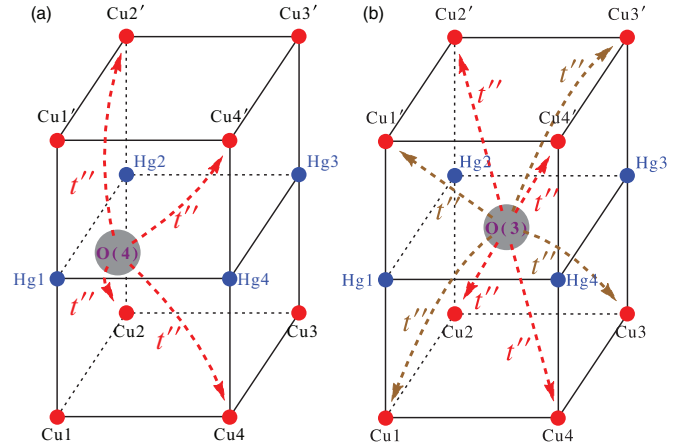


FIG. 2. (Color online) The superexchange paths coupling a pair of hole spins on the CuO-2 layers through states of the intervening oxygen dopant. (a) O(4): antibonding Hg1-O(4) state and (b) O(3): $2p\text{-O}(3)$ states weakly hybridized with (Hg1-Hg3) and (Hg2-Hg4) ions.

by solving a small cluster containing the 2×4 -plaquette sites and the antibonding Hg-O state, to give Hilbert space with a total of nine single particle states with eight electrons. To represent the symmetric O(3) dopant we include the pair of orthogonal active O- $2p$, making a cluster with 10 states and 10 electrons. In each case the cluster is small enough that it can be easily diagonalized. Our aim is to put forward a qualitative explanation of the special properties of Hg1201 listed above, rather than to attempt a numerically accurate description, which would require larger clusters and more detailed parameter estimates.

We begin with the O^d sitting on the O(4) site, displaced towards Hg1 along the diagonal as shown in Fig. 2(a). It forms a Hg1-O(4) bond and only the antibonding state is relevant. An electron can hop from this antibonding state to the O(2) ions (apical oxygen) below and above the Hg plane. Since p_z orbital on O(2) is orthogonal to the $3d_{x^2-y^2}$ on nn Cu1 and Cu1', an electron cannot directly hop onto these sites, but it can hop onto their higher energy $4s$ orbital and then to $2p_x$ and $2p_y$ on the neighboring O(1) planar O ions. The superexchange paths from O(4) that defect to the planar Cu_4 plaquettes are $O(4) \xrightarrow{\text{Hg1}} (\text{Cu2}, \text{Cu4}, \text{Cu2}', \text{Cu4}')$ with

$$H_{O(4)\text{-Cu}} = -t'' \sum_{O \rightarrow i} (c_{i\sigma}^\dagger c_{O\sigma} + \text{H.c.}), \quad (3)$$

where $c_{O\sigma}$ is the electron operator on the O(4) defect site and $O \rightarrow i$ denotes the paths $O(4) \xrightarrow{\text{Hg1}} (\text{Cu2}, \text{Cu4}, \text{Cu2}', \text{Cu4}')$ labeled with dashed red arrows in Fig. 2(a). The potential and interaction terms on the O(4) defect are written as

$$H_{O4} = \epsilon_p \sum_{\sigma} c_{O\sigma}^\dagger c_{O\sigma} + U_p n_{O\uparrow} n_{O\downarrow}, \quad (4)$$

where ϵ_p stands for the energy of the antibonding state relative to the planar on-site energy.

We fix the hopping amplitude into the antibonding Hg-O state and its on-site repulsive interaction as

$$t''/t = 0.5, \quad U_p/t = 1, \quad (5)$$

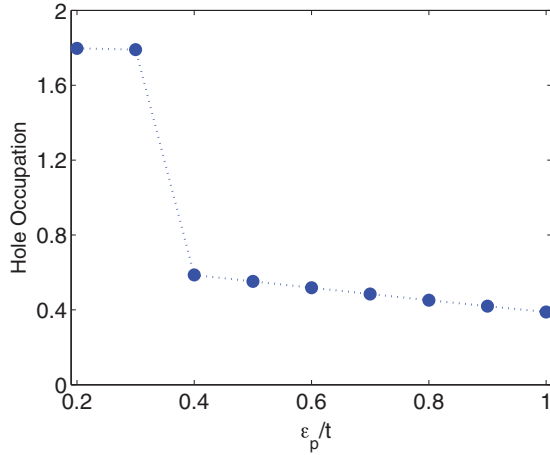


FIG. 3. (Color online) Occupation of holes in the CuO_2 plane for the O(4) defect in Hg1201 as a function of the antibonding state energy ϵ_p .

and tune the oxygen energy position ϵ_p to control the hole occupation in the CuO_2 plane. The total Hamiltonian for the cluster is now obtained by combining the Hubbard term Eq. (1) with the dopant-associated terms Eqs. (3) and (4).

After diagonalizing the Hamiltonian, for small values of ϵ_p , the O(4) site is found to be almost fully filled by electrons and two holes are almost completely injected into the nearby Cu_4 plaquettes as illustrated in Fig. 3. The system can be approximated as two weakly coupled $S = 1/2$ states, resulting in nearly degenerate singlet and triplet states. In this case, the dopant induced charge and magnetic inhomogeneities are similar. With increasing ϵ_p , the occupation of holes in the CuO_2 planes decreases and only a smaller fraction of the holes are injected into the planar sites, as found by Jorgensen and collaborators [7]. Such behavior is also confirmed in our LDA calculations (see Fig. 1). In this case the spin correlations of the two holes increase due to the stronger superexchange path via the O(4) defect.

The ϵ_p -dependent occupation of holes in the twin Cu_4O_4 plaquettes is shown in Fig. 3. The hole occupation dramatically changes around $\epsilon_p/t = 0.3$ implying a level crossing in the ground state. The ϵ_p -dependent energy levels are shown in Fig. 4(a). When $\epsilon_p/t \geq 0.4$, the singlet turns out to be the ground state and the lowest excited states are triplets. The two lower triplets start to separate from the higher energy levels. At $\epsilon_p/t = 0.6$, our parameter set gives the hole occupation in the CuO_2 planes as 0.44 hole per oxygen defect and the two triplets have the energy 39 and 46 meV when $t = 0.43$ eV. Note, a larger but still strongly reduced hole density was reported by Jorgensen *et al.* [7]. The two triplet modes differ in local spin correlations. The lower triplet has the spin correlation $\langle \mathbf{S}_{\text{Cu}2} \cdot \mathbf{S}_{\text{Cu}2'} \rangle = -0.0354$, and the upper one has the correlation $\langle \mathbf{S}_{\text{Cu}2} \cdot \mathbf{S}_{\text{Cu}2'} \rangle = 0.0970$.

As noted earlier, when doping level increases, the O(3) site occupation starts dominating in Hg1201 [7]. Since the O(3) site is at the center of the Hg square, the main difference between the O(4) and O(3) positions is that the latter has two relevant $2p$ orbitals, which hybridize weakly with a pair of Hg ions. In this case there are two different types of electron

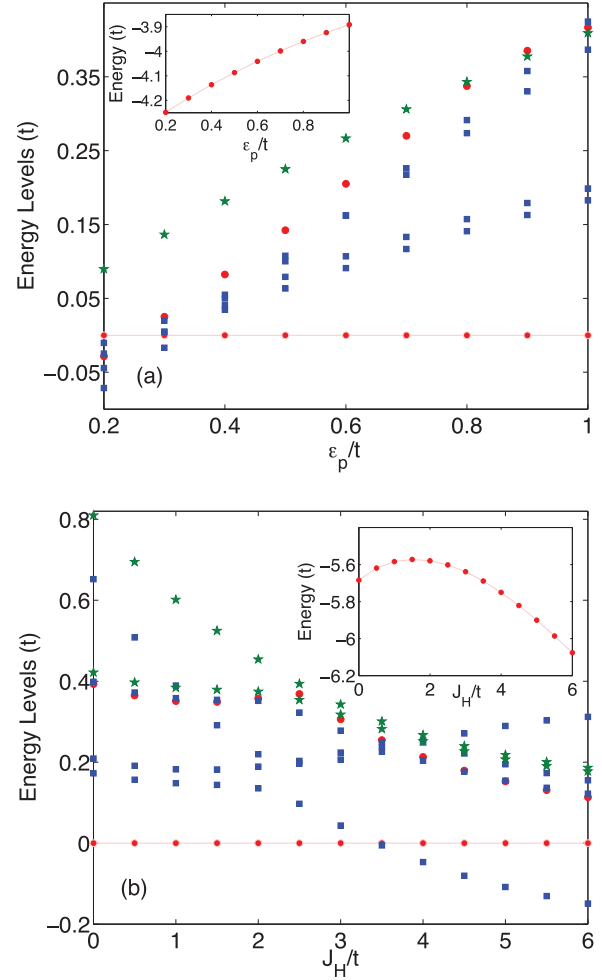


FIG. 4. (Color online) (a) O(4) dopant site: ϵ_p -dependent low energy levels for O(4) defects in the $\text{Cu}_4\text{-O-Cu}_4$ cluster. (b) O(3) dopant site: J_H dependence of the energy levels for O(3) defect with the parameter set in Eq. (8). A solid red circle denotes a singlet state, a solid blue square a triplet, and a solid green star a spin $S = 2$ state. The energy of the reference singlet state is shown in the inset.

superexchange paths: $\text{O}(3) \xrightarrow{(\text{Hg}1, \text{Hg}3)} (\text{Cu}2, \text{Cu}4, \text{Cu}2', \text{Cu}4')$ and $\text{O}3 \xrightarrow{(\text{Hg}2, \text{Hg}4)} (\text{Cu}1, \text{Cu}3, \text{Cu}1', \text{Cu}3')$,

$$H_{\text{O}3\text{-Cu}} = -t'' \sum_{\text{O} \rightarrow i} (c_{i\sigma}^\dagger c_{\text{O}1\sigma} + c_{i\sigma}^\dagger c_{\text{O}2\sigma} + \text{H.c.}), \quad (6)$$

where $\text{O} \rightarrow i$ denotes $\text{O}(3) \xrightarrow{(\text{Hg}1, \text{Hg}3)} (\text{Cu}2, \text{Cu}4, \text{Cu}2', \text{Cu}4')$ and $\text{O}3 \xrightarrow{(\text{Hg}2, \text{Hg}4)} (\text{Cu}1, \text{Cu}3, \text{Cu}1', \text{Cu}3')$ labeled as the red and brown dashed arrows, respectively, in Fig. 2(b). $c_{\text{O}1,2}$ are the electron operators of the two states on O(3) defects.

Since there are two relevant orthogonal states, Hund's rule interaction is relevant on the O(3) defect

$$H_{\text{O}3} = \epsilon_p \sum_{\sigma} (c_{\text{O}1\sigma}^\dagger c_{\text{O}1\sigma} + c_{\text{O}2p,\sigma}^\dagger c_{\text{O}2\sigma}) + U_p (n_{\text{O}1\uparrow} n_{\text{O}1\downarrow} + n_{\text{O}2\uparrow} n_{\text{O}2\downarrow}) + U'_p n_{\text{O}1} n_{\text{O}2} - J_H \mathbf{S}_{\text{O}1} \cdot \mathbf{S}_{\text{O}2}, \quad (7)$$

where U_p and U'_p are for the intraorbital and interorbital interaction and J_H is the Hund's rule interaction. We fix the

parameters as

$$t''/t = 0.5, \quad U_p/t = 1, \quad U'_p/t = 1, \quad \epsilon_p/t = -1, \quad (8)$$

and tune the Hund's rule interaction J_H . The total Hamiltonian for the O(3) dopant is given by a sum of H_0 of Eq. (1) and the two terms Eqs. (6) and (7).

The J_H -dependent energy spectrum for holes around the O(3) defect is shown in Fig. 4(b). For a small value of J_H the ground state is a singlet. With increasing J_H/t , the triplet state decreases in energy and eventually becomes a ground state at $J_H/t \geq 3.5$. At $J_H/t = 4$, there are 1.87 holes on the O(3) defect in the triplet ground state. The spin correlation is $\langle \mathbf{S}_{O1} \cdot \mathbf{S}_{O2} \rangle = 0.208$ implying the parallel alignment of the spins of holes on the O(3) defect as expected according to the standard Goodenough-Kanamori rule. Note, LDA calculations for the O(3) site in Hg1201 [9] and for the same site in the three-layer Hg1223 [15] give a substantial fraction of the doped holes on the site at strong overdoping.

We conclude that in Hg1201 the position of the divalent O^d site, situated in the Hg layer halfway between two CuO_2 layers, strongly changes the magnetic and spin properties relative to the standard case of a singly charged dopant next to a single CuO_2 layer. Our analysis shows that at underdoping, when the oxygen defect is mainly at the asymmetric O(4) site, the superexchange interaction between dopant holes through the O(4) defect leads to a singlet ground state with no RKKY magnetic coupling to Cu nuclei. This gives a natural explanation of the striking difference between charge

and magnetic inhomogeneities in the NMR experiments in Hg1201 [1–4]. Above the singlet ground state, there are two triplet excited states, which are characterized by the different local spin correlations between the nearby CuO_2 planes. The numerical result from the small cluster however underestimates the nonlocal effects, such as the effect of finite hole concentrations in the CuO_2 planes. With the parameter values we have chosen, there are two triplet modes with excitation energies 39 and 46 meV. These energies are of the same order as the values measured in the neutron scattering experiments [5,6].

Lastly, it is worth noting that the NMR experiments did not find AF order down to the lowest doping of $\sim 5\%$. This value is well below estimates for the critical doping for the onset of coexisting superconducting and AF order in an ideal single layer, deduced from NMR experiments on the multilayer Hg-cuprates [16,17] and from theory [18]. This suppression of the AF QCP to very low hole densities ($< 5\%$) in Hg1201 does not weaken superconductivity, which shows a $T_c = 50$ K at 5% density [1]. As these authors remark, the suppression of low energy spin excitations can enhance T_c in a spin fluctuation approach to superconductivity [19].

We used the ALPS [20] to carry out the sparse diagonalizations in this paper [21]. We are grateful to L. Wang for his help with the ALPS package, and to N. Spaldin for giving access to the VASP license. We also thank M. Greven and M. Sigrist for useful discussions. The work in Switzerland was supported by the Swiss Nationalfonds.

-
- [1] Y. Itoh, T. Machi, S. Adachi, A. Fukuoka, K. Tanabe, and H. Yasuoka, *J. Phys. Soc. Jpn.* **67**, 312 (1998).
- [2] D. Rybicki, J. Haase, M. Greven, G. Yu, Y. Li, Y. Cho, and X. Zhao, *J. Supercond. Novel Magn.* **22**, 179 (2009).
- [3] J. Haase, D. Rybicki, C. P. Slichter, M. Greven, G. Yu, Y. Li, and X. Zhao, *Phys. Rev. B* **85**, 104517 (2012).
- [4] D. Rybicki, J. Haase, M. Lux, M. Jurkutat, M. Greven, G. Yu, Y. Li, and X. Zhao, [arXiv:1208.4690](https://arxiv.org/abs/1208.4690).
- [5] Y. Li, V. Baledent, G. Yu, N. Barisic, K. Hradil, R. A. Mole, Y. Sidis, P. Steffens, X. Zhao, P. Bourges, and M. Greven, *Nature (London)* **468**, 283 (2010).
- [6] Y. Li, G. Yu, M. K. Chan, V. Baledent, Y. Li, N. Barisic, X. Zhao, K. Hradil, R. A. Mole, Y. Sidis, P. Steffens, P. Bourges, and M. Greven, *Nat. Phys.* **8**, 404 (2012).
- [7] J. Jorgensen, O. Chmaissem, J. Wagner, W. Jensen, B. Dabrowski, D. Hinks, and J. Mitchell, *Phys. C: Supercond.* **282-287**, 97 (1997).
- [8] E. V. Antipov, A. M. Abakumov, and S. N. Putilin, *Supercond. Sci. Technol.* **15**, R31 (2002).
- [9] C. Ambrosch-Draxl, P. Süle, H. Auer, and E. Y. Sherman, *Phys. Rev. B* **67**, 100505 (2003).
- [10] Supercell calculations were performed in VASP [22] *ab initio* package using PAW method [22,23]. For the DOS calculations illustrated in Fig. 1 an energy cutoff of 400 eV with Γ -centered k -point mesh of $10 \times 10 \times 8$ and experimental lattice constants [24] were used.
- [11] F. C. Zhang and T. M. Rice, *Phys. Rev. B* **37**, 3759 (1988).
- [12] M. S. Hybertsen, E. B. Stechel, M. Schluter, and D. R. Jennison, *Phys. Rev. B* **41**, 11068 (1990).
- [13] Y. Nagaoka, *Phys. Rev.* **147**, 392 (1966).
- [14] Y. Itoh, M. Matsumura, and H. Yamagata, *J. Phys. Soc. Jpn.* **66**, 3383 (1997).
- [15] D. J. Singh and W. E. Pickett, *Phys. Rev. Lett.* **73**, 476 (1994).
- [16] H. Mukuda, S. Shimizu, A. Iyo, and Y. Kitaoka, *J. Phys. Soc. Jpn.* **81**, 011008 (2012).
- [17] W.-Q. Chen, J. Y. Gan, T. M. Rice, and F. C. Zhang, *Europhys. Lett.* **98**, 57005 (2012).
- [18] A. Himeda and M. Ogata, *Phys. Rev. B* **60**, R9935 (1999).
- [19] Y. Ohashi and H. Shiba, *J. Phys. Soc. Jpn.* **62**, 2783 (1993).
- [20] B. Bauer, L. Carr, H. Evertz, A. Feiguin, J. Freire, S. Fuchs, L. Gamper, J. Gukelberger, E. Gull, S. Guertler *et al.*, *J. Stat. Mech.: Theory Exp.* (2011) P05001.
- [21] <https://alps.comp-phys.org>.
- [22] G. Kresse and J. Furthmüller, *Comput. Mater. Sci.* **6**, 15 (1996).
- [23] G. Kresse and D. Joubert, *Phys. Rev. B* **59**, 1758 (1999).
- [24] Q. Huang, J. W. Lynn, Q. Xiong, and C. W. Chu, *Phys. Rev. B* **52**, 462 (1995).